# Drift velocity partitioning indicates anomalous high westward drift component for the Indian plate during ~65 ± 2 Ma

Amarjeet R. Bhagat[1], S. J. Sangode[1], Ashish Dongre[1]

[1]Department of Geology, Savitribai Phule Pune University, Pune, India

**Corresponding author: Satish Sangode (sangode@unipune.ac.in)**

This is a non-peer reviewed preprint. This manuscript is submitted for publication in JOURNAL OF GEODYNAMICS. Subsequent version of this manuscript may differ slightly in content. Once accepted, the published version will be made available through the 'peer-reviewed publication doi'.

## Key Points:

- **Very high drift rates for the Indian subcontinent at ~65 Ma result from Plume-Lithosphere interaction during the Deccan Trap eruption.**
- **A combination of plate driving forces explain the geodynamics of the high drift rates.**
- **Significant contribution from the Indian plate lithospheric root delamination is proposed.**


## Abstract

**Rapid northward drift of the Indian plate after 130 Ma has also recorded significant plate rotations due to the torques resulting from multiple vector force components. Seismic tomography of the Indian Ocean and palaeomagnetic database of the Deccan Traps are used here to constrain drift velocities at different temporal snapshots, resulting into estimates of 263.2 to 255.7 mmyr$^{-1}$ latitudinal drift, 234 to 227.3 mmyr$^{-1}$ longitudinal drift and 352.2 to 342.1 mmyr$^{-1}$ diagonal drift, for the period from ~66 to 64 Ma during the Chrons C30n.y–C29n.y. Alternative displacement models suggest active driving forces arising from *i)* slab pull, *ii)* ridge push from eastern-, western and**

**southern plate margins, and *iii)* Reunion plume-push force; in addition to delamination of the lithospheric root during approximately 65±2 Ma. Delamination of the root amplified the buoyancy of the Indian plate in contrast to sudden loading from Deccan basaltic pile that resulted into complex drift dynamics expressed by hyper plate velocities with an anomalous westward drift component of >342 mmy$^{-1}$.**

## Plain Language Summary:

**Northward drift of India after rifting from Australia-Antarctica around 130 Ma has been well constrained from the marine magnetic anomaly records preserved in the Indian ocean. Except for chron C34n where the magnetic polarity remained constant for an exceptionally longer period of time, we do not find any lapses in the recorded history for the drift of Indian subcontinent. The sea floor acts as a historical record keeper for the plate motions of the past 180-200 Ma. Despite this well-maintained decorum, there appear to be certain events that escape preservation in the global conveyor belt and may not be**

**reflected in the anomaly records. Here, we present a hitherto unnoticed-unreported event during the Deccan Volcanism from magnetic anomaly database; which however, is clearly visible in paleomagnetic data of the Deccan Traps. It is well established that the highest plate velocities that can be achieved by drifting plates range around 180-200 mmyr$^{-1}$. However, in the present study based on paleomagnetic data, we present drift rates that are in excess of 300 mmyr$^{-1}$. These drift rates result from contemporary existence of multiple plate driving forces that acted with varying intensities on the Indian plate during the Deccan event. Slab pull combined together with plume push, ridge push and lithospheric root delamination propelled the Indian plate at tremendously high velocities which resulted in multiple course corrections within a short span of ~1.5 Ma.**

# Introduction:

Indian plate presents one of the most dynamic trajectories of plate motion by its rapid northward drifts and clockwise/anticlockwise rotations (Patriat and Acache 1984, Eagles and Hoang 2013, O'Neill et al 2003). Multiple surges in the plate velocities are recorded at 130, 85 and 65 Ma (Van Hinsbergen et al 2011, Eagles and Hoang 2013, Gibbons et al 2013, Gibbons et al 2015, Jagoutz et al 2015, Cande et al 2010, Cande and Stegman 2011, Demets and Merkouriev 2021,

Eagles and Wibisono 2013) and are related to the plate encounters with three well defined mantle plumes. The 130 Ma event was caused by the Kerguelen plume forming the Rajmahal traps in India (Kale 2020, Ghatak and Basu 2011, Taludkar and Murthy 1971) , Bunbury basalts in Australia (Frey et al 1996, Ingle et al 2002, Zhu et al 2009, Olierook et al 2016) and Kerguelen plateau in the Southern Indian Ocean. This resulted in rifting of India from East Gondwana (Aitchison et al 2007, Acharyya 2000, Argus et al 2011, Bardintzeff et al 2010) forming the Indian subcontinental block comprising (India + Madagascar + Seychelles). This rifting was followed by the Marion plume arrival at the End Cretaceous (~90-85Ma) (Torsvik et al 1998, Georgen et al 2001, Storey 1995), resulting in separation of India + Seychelles block from Madagascar.

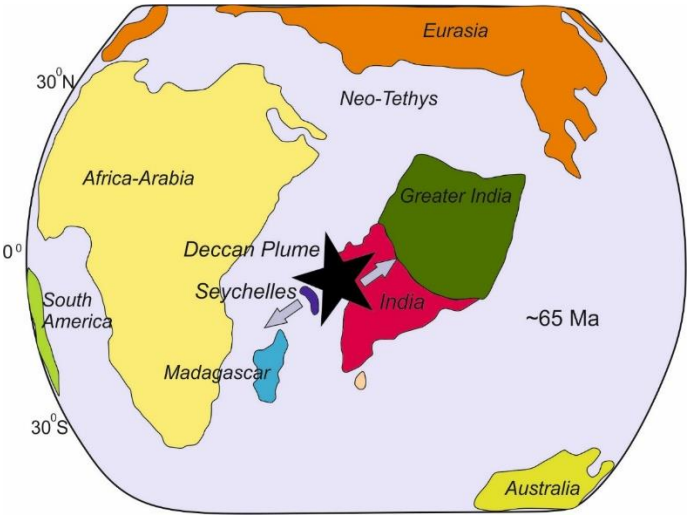


**Fig 1. Position of the Indian subcontinent during the Deccan LIP eruption event at 65 Ma redrawn after Van Hinsbergen et al (2011).**

The final Reunion plume encounter led to India-Seychelles separation and eruption of the Deccan flood basalts at ~65.5 Ma (Sangode et al 2022, Vandamme

et al 1991, Jay and Widdowson 2006, Chenet et al 2007, Chenet et al 2008). Drift rates for the Indian subcontinent during each of these events are well constrained, with the Deccan event displaying the highest recorded plate velocities. However, it is possible that these velocities do not represent an upper limit on the velocities of drifting continents as proposed by Zahirovic et al (2015), wherein they concluded that the maximum possible velocities range around 150-200 $mmyr^{-1}$. We present here drift rates calculated from declination and inclination differences between the initial and final positions of the Indian subcontinent during the Deccan episode. These calculations were made possible by analysing the palaeomagnetic database of Sangode et al (2022) who compiled previous studies done on the Deccan Traps and provided a new improved Deccan Superpole. The generated database went through extensive statistical and analytical filtering resulting into a robust repository of the paleomagnetic data for the Deccan Traps.

In the following sections we present a comparison between two end member scenarios for the Deccan event based on paleomagnetic data. Model 'A' presents the results based on the analysis of the Central Tendency Data. This model builds upon the conventionally accepted convergence for India with respect to Eurasia. Model 'B' assesses the results from the analysis of Filtered Mean Data, presenting major shifts in convergence direction possibly induced by the combined of slab pull of the Neo-Tethys slab, ridge push emanating from the western-southern-eastern spreading centres, plume push of the Reunion mantle

plume and delamination-decoupling of the lithospheric root beneath the Indian subcontinent. Once the possible causes for the observed drift rates are explained, we propose the position of the delaminated root of the Indian subcontinent within the upper mantle. This discovery opens new vistas and expands our understanding of plume-lithosphere interactions along with the possible fate of thermally eroded lithospheric roots of Archean cratons.

## Drift, rotation and tilt of the Indian plate

From the marine magnetic anomaly records, it is evident that the Indian subcontinent moved at extreme high velocities during the period from C32 to C28 with peak values ranging from ~185- 200 mm/yr recorded during Chron C29r (Cande and Stegman 2011, Pusok and Stegman 2020, Sangode et al 2022, Rodriguez et al 2021, Van Hinsbergen et al 2015). These drift velocities are very high when compared with the fastest spreading rates obtained from the East Pacific Rise (~140mm/yr) existing today (Lonsdale 1977, Clennett et al 2020). These high drift velocities for the Indian subcontinent have been classically attributed to its interaction with the Reunion plume during the Deccan eruption event, which amplified the existing velocity pattern of the Indian plate. Still the velocities are averaged out hiding any anomalous rates between the age benchmarks.

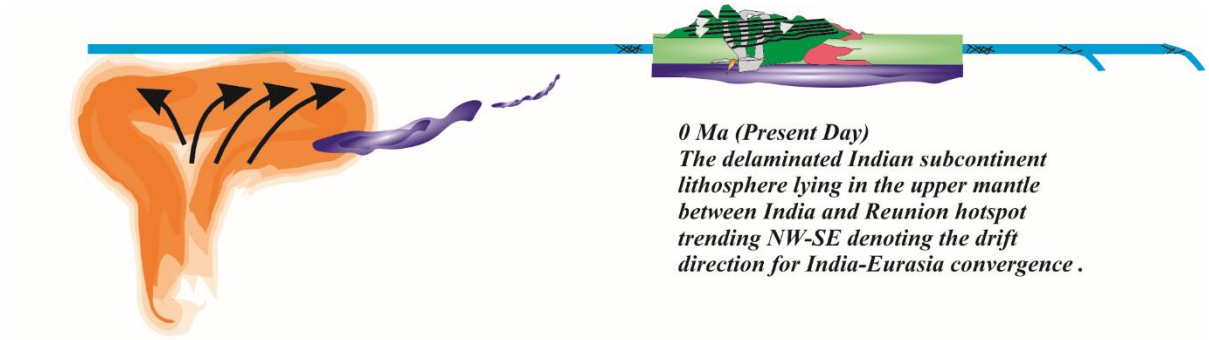

*0 Ma (Present Day)*
*The delaminated Indian subcontinent lithosphere lying in the upper mantle between India and Reunion hotspot trending NW-SE denoting the drift direction for India-Eurasia convergence .*

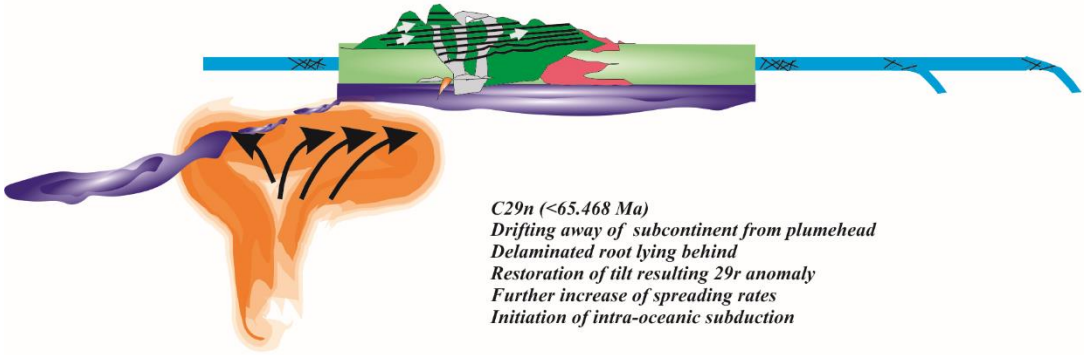

*C29n (<65.468 Ma)*
*Drifting away of subcontinent from plumehead*
*Delaminated root lying behind*
*Restoration of tilt resulting 29r anomaly*
*Further increase of spreading rates*
*Initiation of intra-oceanic subduction*

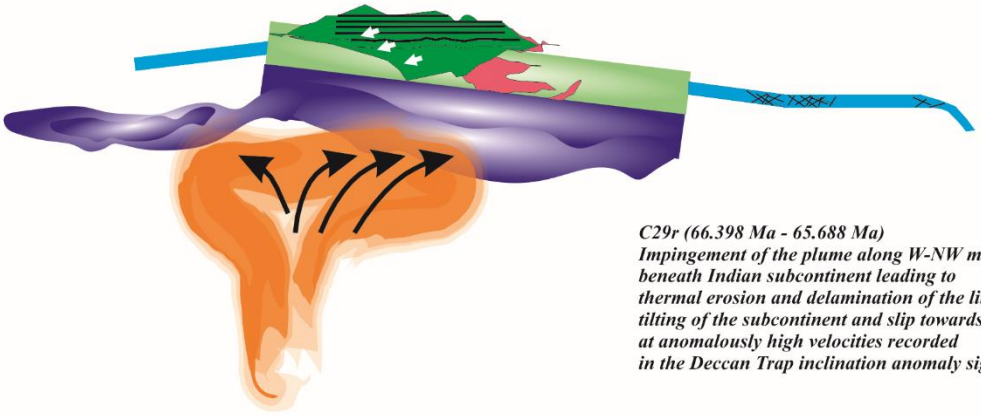

*C29r (66.398 Ma - 65.688 Ma)*
*Impingement of the plume along W-NW margin beneath Indian subcontinent leading to thermal erosion and delamination of the lithosphere tilting of the subcontinent and slip towards NW at anomalously high velocities recorded in the Deccan Trap inclination anomaly signature*

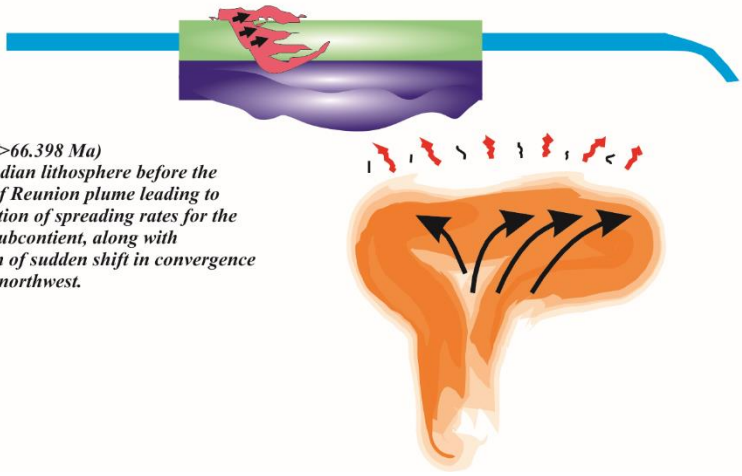

*C30n.y (>66.398 Ma)*
*Thick Indian lithosphere before the arrival of Reunion plume leading to acceleration of spreading rates for the Indian subcontient, along with initiation of sudden shift in convergence towards northwest.*

**Fig 2. The mechanism of Deccan inclination anomaly modified after Sangode et al (2022). At C30n the plume-head arrives beneath the Indian subcontinent resulting in minor alkaline intrusives. This is followed by the main phase of eruption at C29r which led to tilting of the Indian subcontinent towards north by ~10º, along with the delamination of the lithospheric root below the subcontinent. The root delamination led to an increase in buoyancy, further contributing to the anomalous drift rates and slip towards NW. At C30n, the subcontinent moved away from the plume-head, restoring normal inclination values along the northeastwardly march of Indian subcontinent.**

Primarily, the drift rates are calculated from the Marine Magnetic Anomalies (MMA) in the ocean basins; however, in situations where anomaly data are sparse the drift rates are calculated from paleomagnetic measurements based on land values. Present work is built up on the database of Sangode et al (2022), who discovered the Deccan inclination anomaly from a compilation and analysis of existing paleomagnetic data from the Deccan Traps. They discovered that the paleomagnetic inclinations for the chrons C30n, C29r and C29n differ significantly for such a short-time span, with C29r depicting highly anomalous inclination values. This inclination anomaly was attributed to the ~10º tilt of the Indian plate towards north leading to short episode of epicontinental marine transgression along the Narmada rift (Kumari et al 2020, Keller et al 2021). This tilt is attributed to the arrival of the Reunion plume at the NW-W periphery of the Indian subcontinent resulting in uplift of southern tip of peninsular India and dipping of the northern edge of the subcontinent for a very brief time spanning

C29r. The tilt was restored back to normal during C29n, resulting in normal inclination values for the same.

## Constrains from paleomagnetic database

Statistical analysis of the paleomagnetic data leads to two end member models which contrast not only in position but also significantly differ in the drift velocities for the Indian subcontinent. 'Model A' explains the results obtained from Central tendency data, while 'model B' explains the results obtained from the Filtered mean data. As it is unclear when the Deccan volcanism event precisely initiated, we have considered the initial position of the Indian subcontinent for our calculations at the end of Chron C30n while the final position at the end of C29n signifying the end of main phase eruption of Deccan tholeiites. This provides us with a ~1.5 Ma (1.518 Ma for GTS2020; 1.563 for MQSD20) time window to monitor the movements of the Indian subcontinent spanning C29r and C29n. Co-ordinates for the city of Nagpur in Central India were used as a reference point for calculating movement of Indian plate.

| | Chron 30n.y | | C29r.y | | C29n.y | |
|---|---|---|---|---|---|---|
| | D | I | D | I | D | I |
| Central Tendency | 333 | -38 | 157 | 47 | 341 | -32 |
| Window | 297-366 | 20-56 | 121-193 | 29-65 | 305-377 | 14-50 |

| | | | | | | |
|---|---|---|---|---|---|---|
| Mean after applying the Filter. | 338 | -38.7 | 153.3 (333.3 antipode) | 47.4 | 334.8 | -35.1 |
| Scatter | α-95: 2.5; k = 21.37, N:153 | | α -95: 1.1, k = 36.05, N: 451 | | α -95: 4.3, k:21.61, N: 54 | |
| Anomaly with Vandamme *et al.* 1991 | +4 (clockwise) | -5 (shallow) | -0.7 (anti-clockwise) | +5 (deeper) | +0.8 (clockwise) | -8 (shallow) |
| Anomaly with Réunion latitudes* | | $+1^0$ | | $+10^0$ | | $-2^0$ |

**Table 1: Data table showing the results obtained after statistical treatment of paleomagnetic data.**

For 'model A' (Central tendency data), the D/I values for C30n.y. are 333/-38 and 341/-32 for C29n.y. The initial position of the Indian subcontinent at C30n.y is exactly southwest of the final position at C29n.y. This agrees well with the established literature, except for the fact that the displacement of India for the specified time period is massive. The differences in initial and final positions depict a latitudinal drift of 6°N and a longitudinal drift of 8°E. Simple trigonometric calculations reveal a diagonal drift of about 10°NE which is colossal when compared with the highest drift rates that have been recorded for India-Eurasia convergence. Assuming 1° = 111 km, latitudinal, longitudinal and

diagonal drifts can be calculated as 666 km N, 888 km E and 1110 km NE respectively. These results when compared with the above-mentioned timespan, evolve into drift rates which have not been directly documented earlier. These are presented in Table 2 and figure 3.

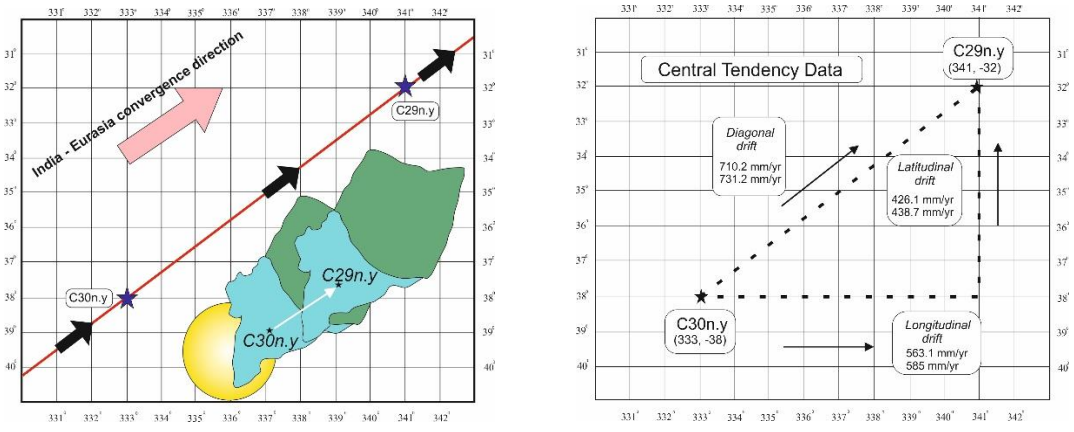


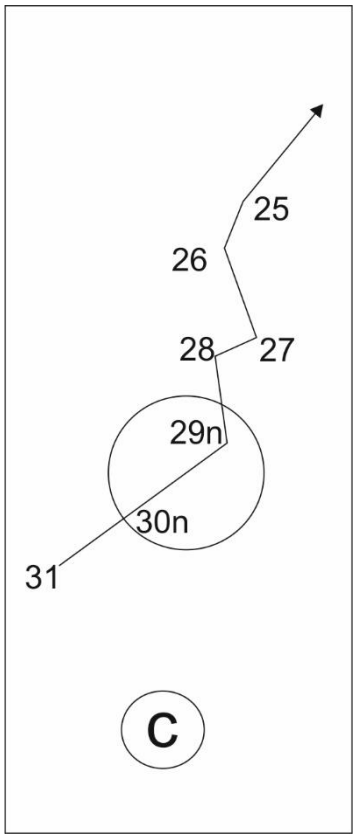


**Fig 3. Model A: North-eastward drift of the Indian subcontinent can be observed along with the calculated drift rates based on inclination data. a) The blue stars indicate initial**

**and final positions for the Indian subcontinent during the chrons C30n.y and C29n.y. The black arrows point the directions of drift calculated from the present study. The larger grey arrow indicates the established convergence direction of Indian subcontinent with respect to Eurasia, while the red line marks the trace of the drift direction as deduced from the paleomagnetic data. The yellow circle represents Reunion plume, blue portion indicates the present day extent of Indian subcontinent and the green portion indicates subducted continental part of Greater India. The small black stars represent the position of present day city of Nagpur in central India, which was used as a reference point to conduct the calculations. The small white arrow depicts the relative motion of the subcontinent at initial and final positions, showing the northeastward drift of India. b) The black stars mark the initial and final positions of the Indian subcontinent. Longitudial (563.1 and 585 mmyr$^{-1}$), latitudinal (426.1 and 438.7 mmyr$^{-1}$ ), and the diagonal (710.2 and 731.2 mmyr$^{-1}$ ) drift rates have been calculated by extrapolating the vectors from initial and final positions along respective directions. Two different spreading rates result from using the dates for chrons C30n.y and C29n.y for MQSD20 and GTS 2020, where the above mentioned period spans 1.518 and 1.563 Ma respectively, resulting higher drift rates for MQSD20 and slightly lower rates for GTS2020. c) Established plate motion direction for India-Eurasia convergence, with the numbers denoting Anomaly sequences. The circle depicts the timespan considered for the present study spanning C30n-C29n, while the numbers denote Magnetic chrons. The results predicted by 'Model A' follow this established APW trend for India very precisely.**

'Model B' (Filtered mean data) however indicates an altogether different result. The D/I values are 338/-37.8 and 334.8/-35.1 respectively for the final and initial positions (i.e., C30n.y and C29n.y). This presents smaller drift rates when

compared with ‘model A’. However, there appears to be some sort of disparity when analysing the drift directions. The final and initial positions differ in the convergence trend that is generally accepted for India-Eurasia. The subcontinent appears to have moved towards northwest with respect to its initial position at C30n.y. This is in contrast with the results from ‘model A’ which shows a northeast convergence for the above-mentioned timespan. The drift values calculated from the initial and final positions reveal 3.6° N latitudinal, 3.2°W longitudinal and 4.82° NW diagonal drifts respectively for the ‘model B’. These values equate to displacements of 399.6 km, 355.2 km and 534.65 km respectively and are shown in Table 2 and figure 4.

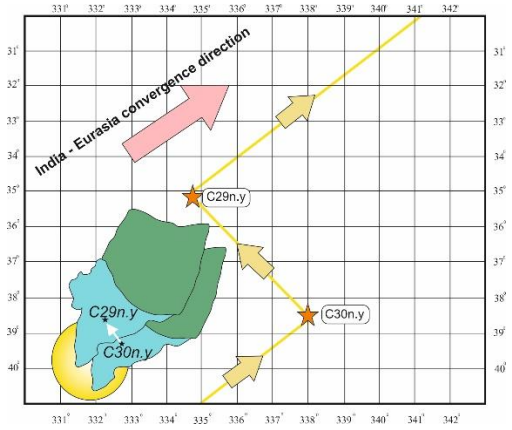


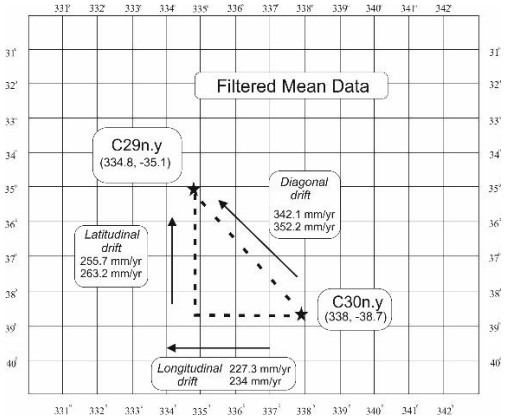

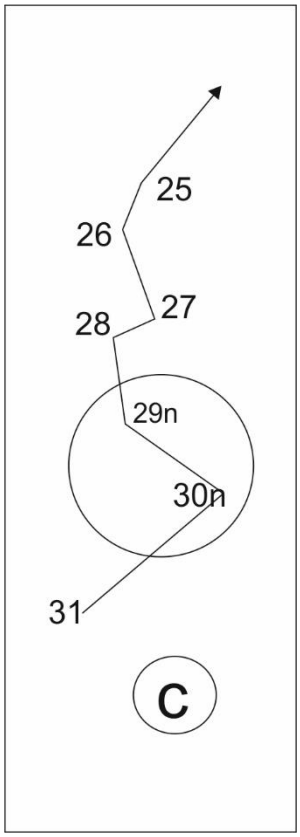


**Fig 4. Model B: North-westward drift of the Indian subcontinent observed along with the calculated drift rates based on inclination data. *a)* The orange stars indicate initial and final positions for the Indian subcontinent during the chrons C30n.y and C29n.y. The smaller arrows point the direction of drift calculated from the present study. The larger grey arrow indicates the established convergence direction of Indian subcontinent with respect to Eurasia, while the yellow line marks the trace of the drift direction as deduced from the paleomagnetic data. The yellow circle represents the Reunion plume, blue portion indicates the present day extent of Indian subcontinent while the green portion indicates subducted continental Greater India. The small black stars represent the position of present day city of Nagpur in central India, which was used as a reference point to conduct the calculations. The small white arrow depicts the relative motion of the subcontinent at initial and final positions. It can obeserved clearly that the northeastward motion of India was interrupted when it encountered the Reunion plume**

**at ~65Ma leading to a change of convergence direction at anomalously high velocities. The model thus predicts that the plume push emanating from the Reunion plume did overcome the slab pull and ridge push forces acting on the Indian plate during its encounter for a short period of time. This change in direction was corrected once the Indian subcontinent moved away from the sphere of direct influence of the Reunion plume. *b)* The black stars mark the initial and final positions of the Indian subcontinent. Longitudial (227.3 and 234 mmyr$^{-1}$ ), latitudinal (255.7 and 263.2 mmyr$^{-1}$ ), and diagonal (342.1 and 352.2 mmyr$^{-1}$ ) drift rates have been calculated by extrapolating the vectors from initial and final positions along respective directions. Two different spreading rates result from using the dates for chrons C30n.y and C29n.y for MQSD20 and GTS 2020, where the above mentioned period spans 1.518 and 1.563 Ma respectively, resulting higher drift rates for MQSD20 and slightly lower rates for GTS2020. c) The figure shows APW path calculated for the India-Eurasia covergence based on 'Model B'. The circle depicts the time spanning between C30n and C29n, while the numbers denote the magnetic chrons. Starting C30n a deviation towards Westward from the established NE trend is observed which is restored at C29n.**

The high drift rates can be attributed to various factors, most prominent being the convergence of India towards Eurasia owing to the multiple subduction zones present at the southern Eurasian margin (Aitchison et al 2000, Aitchison and Davis 2004, Baxter et al 2016, Bouilhol et al 2013, Gibbons et al 2015, Buckman et al 2018). The enormous slab pull experienced by the Indian plate towards north from the subducting Neo-Tethyan slab has been postulated by many to be the major driver of rapid movement of India. This could possibly be the case if the lithospheric plate experiencing slab pull was entirely oceanic in

character and did not carry significant continental landmass such as India (Pusok and Stegman 2020, Van Hinsbergen et al 2015, Zahirovic et al 2012). The negative buoyancy of the Indian subcontinent could possibly not have allowed such a high drift rate based merely on slab pull of the downgoing oceanic slab attached to the Indian plate (Forsyth and Uyeda 1975, Morgan and Parmentier 1984).

| | Central Tendency (Latitudinal drift) | Filtered Mean (Latitudinal drift) | Central Tendency (Longitudinal drift) | Filtered Mean (Longitudinal drift) | Central Tendency (Diagonal drift) | Filtered Mean (Diagonal drift) |
|---|---|---|---|---|---|---|
| Distance covered in degrees | $6^0$ | $3.6^0$ | $8^0$ | $3.2^0$ | $10^0$ | $4.82^0$ |
| Distance covered in kilometres | 666 km | 399.6 km | 888 km | 355.2 km | 1110 km | 534.65 km |
| Spreading rate (GTS 2020) | 426.1 mm $yr^{-1}$ | 255.7 mm $yr^{-1}$ | 563.1 mm $yr^{-1}$ | 227.3 mm $yr^{-1}$ | 710.2 mm $yr^{-1}$ | 342.1 mm $yr^{-1}$ |
| Spreading rate | 438.7 mm $yr^{-1}$ | 263.2 mm $yr^{-1}$ | 585 mm $yr^{-1}$ | 234 mm $yr^{-1}$ | 731.2 mm $yr^{-1}$ | 352.2 mm $yr^{-1}$ |

| | | | | | | |
|---|---|---|---|---|---|---|
| (MQSD20<br>) | | | | | | |

**Table 2. Calculated drift rates from the inclination data for Central tendency and filtered mean data respectively for GTS2020 and MQSD2020 timescales.**

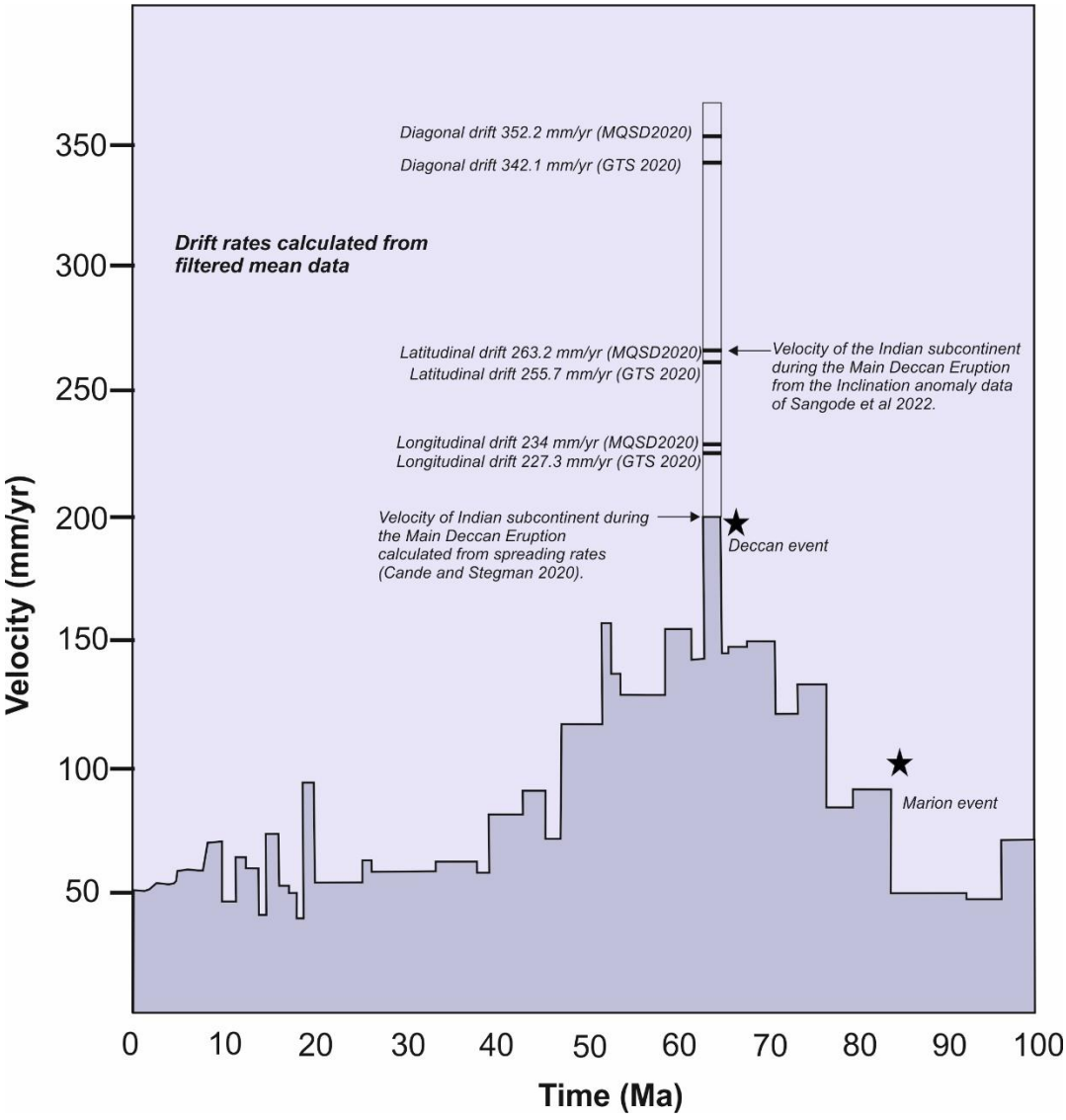


**Fig 5. A plot showing spreading rates versus time of the Indian plate for the past 100 Ma modified after White and Lister (2012). At the Deccan event, the new data has**

**been plotted to depict the newly discovered drift rates from the filtered mean data for the Indian Subcontinent. The black stars mark mantle plume events. The drift rates for the Indian subcontinent peak at the Deccan event, following which there is a considerable decrease in drift rates. This has been attributed to the moving away of the subcontinent from the Reunion hotspot leading to increasing viscosity of the asthenosphere beneath the Indian subcontinent acting as an obstruction to the rapid drift.**

## Slab pull or Ridge push?

Amongst the forces acting over the Indian plate during Late Cretaceous, slab pull appears to be the major driver; as the velocity of a drifting plate is directly proportional to the length of subduction zone attached to it. This is evident, as there existed a long subduction zone all along the southern Eurasian margin. This more than ~10,000 km long subduction zone would have acted as a major driver for the plate motion of India since its rifting from Madagascar (~85-90 Ma), only to be modulated/interrupted by the Reunion plume (67-64 Ma). Multiple models of subduction systems have been proposed for the Neo-Tethyan subduction system existing between India and Eurasia during the End-Cretaceous. The presence of island arcs adds to the slab pull factor by proposing the existence of multiple intra-oceanic subduction systems in the Neo-Tethyan realm (Bouilhol et al 2013, Replumaz et al 2019, Jagoutz et al 2015, Aitchison et al 2007, Searle 2019).

The western spreading centre in the Mascarene basin being younger would have been more vigorous and thereby have a dominant role in driving the Indian plate after the India Madagascar separation as compared to the eastern spreading centre in the Wharton Basin during the Late Cretaceous (Bhattacharya and Yatheesh 2015, Nemcok et al 2016, Dyment 1993, Dyment 1998). Further the cessation of spreading in the Mascarene basin coupled together with the ridge jump onto the proto-Central Indian Ridge led to enhancement of spreading rates in the Central Indian Ocean Basin, and finally the opening of the Carlsberg ridge at the end of the Deccan event accompanying the India-Seychelles separation adds even more impetus to the North-eastward drift of the Indian subcontinent (Bhattacharya and Yatheesh 2015, Merkouriev and Sotchenova 2003).

This coupling of the plate driving forces i.e., the push emanating from the southern spreading centre (Southeast Indian Ridge) and the western spreading centre (Central Indian Ridge) (Dyment 1993,1998), the slab pull from the north (Tethyan subduction system) would have resulted in a predominantly northerly–northeasterly drift of the Indian subcontinent (Patriat and Acache 1984).

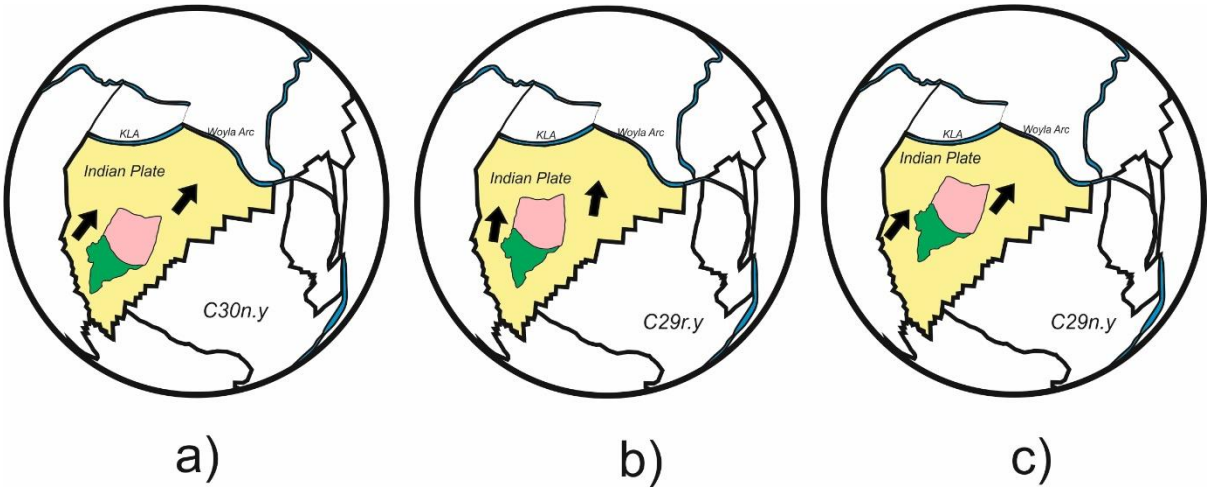


**Fig 6. Arrangement of the plate boundaries for Indian plate at time of interaction with the Reunion plume (after Gibbons et al 2015). The convergence directions for C29r depicting a slight change for the Indian subcontinent which was restored substantially back to normal after the Deccan event.**

However, based on the analysis of the Declination data in 'model B', it appears that this dominant drift direction might have been affected severely or changed altogether although for a short time interval. This implies that a plume head upon interaction with continental lithosphere can significantly affect the directions of plate movement, by overcoming the existing plate driving forces. This is confirmed by the lithospheric tilting recorded within the DVP (Sangode et al 2022), which depicts that the incipient plume push arising from the first interaction of a deep-seated mantle plume with continental lithosphere can result in tilting of the continental block. Along with this tilting there appears to be an additional sideways component associated, more likely to result in the sideward drift/slip with velocities that surpass existing plate tectonic speed limits. Thus, the plume push force originating from the Reunion plume not only could have

enhanced the drift velocity of the Indian plate with respect to Eurasia, but it could have also caused a previously unnoticed westward drift/slip during the ~1.5 Ma duration with velocities as high as ~352 mm/yr $^{-1}$.

This is possible as the plume made its first contact along the North-western fringes of the Indian subcontinent thereby resulting in a northward tilting, where maximum mass of the subcontinent was positioned. This concentration of mass towards north is further evident from the tomography cross sections which show maximum thickness of the Indian subcontinent towards north Fig.7. After C30n.y the subcontinent moved beyond the sphere of direct influence of the plumehead, restoring the slab pull (Neo-Tethyan system at the southern margin of Eurasia) and ridge push forces resulting in north-eastward drift of India. The drift rates were however significantly enhanced with renewed push from the Reunion plume resulting in the rates that were higher than what they were before the Reunion encounter, but significantly lower than what it was during the event which lasted about 1.5 Ma.

## Tomographic hunt for the lost root

Another possible explanation for this rapid drift could be attributed to the absence of a thick cratonic root beneath the Indian subcontinent especially along the western margin where the lithospheric thickness is less than 100 km compared to ~150-200 km for rest of the Indian subcontinent (Kumar et al 2007, Dessai and Griffin 2021, Jaupart and Mareschal 1999). This ~100-200 km average thickness

of the Indian cratonic lithosphere is notably less when compared with the global average of 350-450km for Archean cratonic regions (Conrad and Lithgow-Bertelloni 2006).

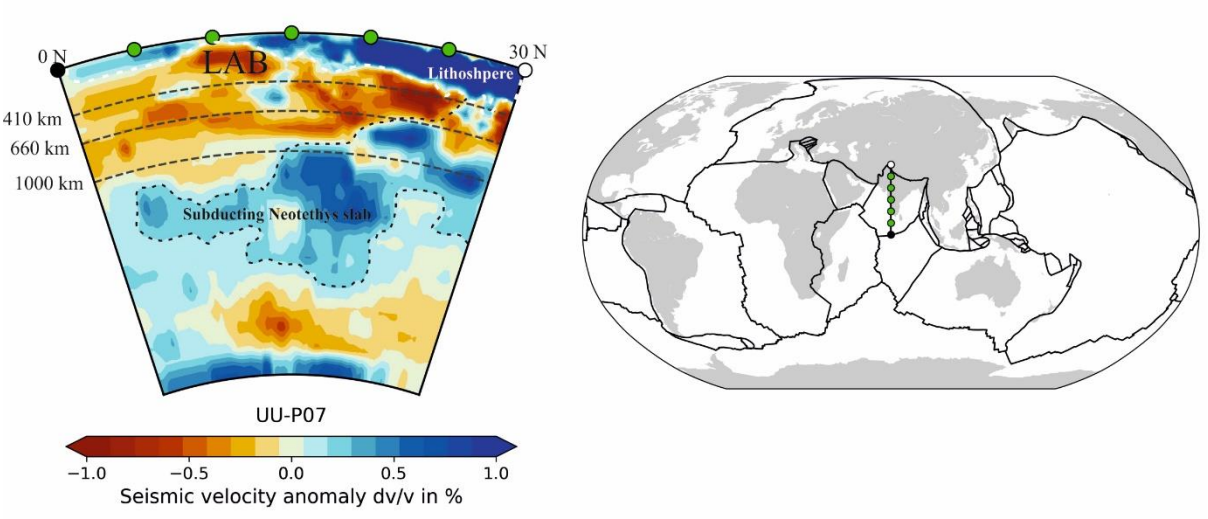


**Fig 7. A seismic tomographic cross section of the upper mantle from the model UU-P07 (Amaru 2007, Hall and Spakman 2015) for the present-day Indian subcontinent through 75°E from 30°N to 0°, showing variable thickness of the lithosphere beneath the Indian subcontinent hinting towards the absence of a deep lithospheric root, which if present would have impeded the plate velocities. The concentric dashed lines mark the seismic velocity discontinuities in the upper mantle. LAB stands for Lithosphere-Asthenosphere boundary. The Indian subcontinental lithosphere in blue is demarcated from the Asthenosphere by the white dashed line. The black dashed enclosure in the lower mantle shows the subducting Neo-Tethyan lithosphere beneath the Indian subcontinent.**

This root deficit can be attributed to thermal erosion by major encounters with mantle plumes within the past 120 Ma along the southern (Marion and Crozet), eastern (Kerguelen) and western (Reunion) margins of the Indian subcontinent (Dessai and Griffin 2021, Griffin et al 2009, Paul and Ghosh 2021, Raval and

374 Veeraswamy 2003). Even the Central Indian region that displays the thickest
375 lithosphere for the Indian subcontinent shows a lithospheric depth of only 200-
376 250 km (Maurya et al 2016).

377 These plume impingement events resulting in thermal erosion and weakening of
378 the base of the lithosphere can lead to mechanical erosion of the lithospheric root
379 further by generating convective stresses in the toroidal mantle flow (Davies
380 1994). The roots act as anchors for the continents in the mantle, once weakened
381 by the plume induced thermal instability, it is difficult to sustain the structural
382 integrity under the elevated thermal gradients. This implies that the lithospheric
383 root can no longer retain its distinct rigidity and slowly gets eroded or deformed
384 by the convective mantle flow. Once this happens it is difficult for the continents
385 to retain the coefficient of friction with the asthenospheric or mantle drag
386 (Stoddard and Abbot 1996, Bredow et al 2017). A buoyant continental mass
387 deprived of its root can prove to be an excellent candidate for this continental
388 "MotoGP".

389 We present vertical cross sections of the mantle by using S-wave tomographic
390 models along a traverse in the Indian ocean between co-ordinates (25°S, 55°E)
391 and (15°N, 75°E). These cross sections have been obtained by using Submachine,
392 an open-source seismic tomography software that hosts a repository of multiple
393 P and S-wave tomography models for the interior of the earth. S-wave models
394 provide better resolution in the upper mantle, which explains the choice of our

models in the present study. The results show a distinct cold-high velocity anomaly at sub-equatorial latitudes in the upper mantle enclosed by lower velocity plume material highlighted by the dashed enclosures.

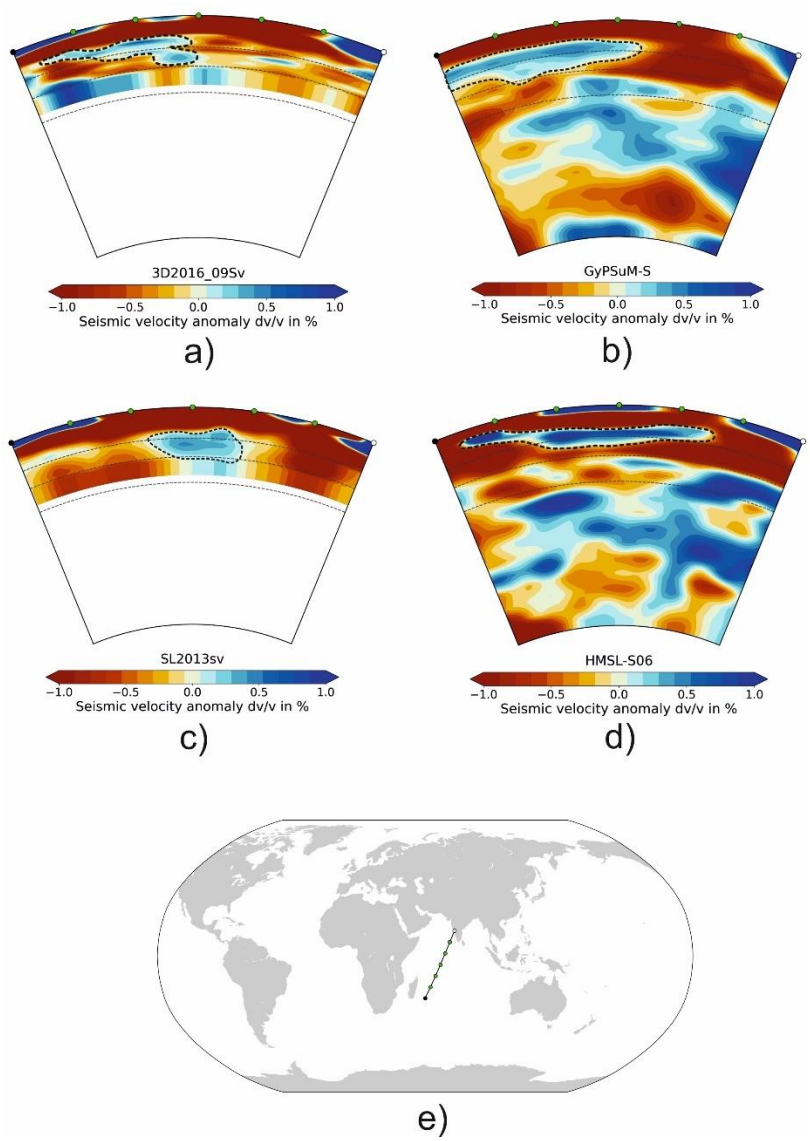


**Fig.8 Seismic tomographic S-wave profiles for the mantle. Cross sections from (25°S, 55°E) and (15°N, 75°E) based on (3D2016_09Sv), (GyPSuM-S), (HMSL-S06) and (SL2013sv), depicting the proposed lithospheric root/keel dislodged from the Indian subcontinent during the Deccan episode.**

The shape of this anomaly does not correspond to a subducted slab of oceanic lithosphere, nor there have been any reported subductions at those latitudes in the past 100 Ma **Fig.9**. We say 100 Ma, as the slab is yet lying in the lower reaches of the mantle transition zone and barely penetrated the lower mantle not ventured below 710 km. The horizontal alignment also defies any chances of a subducted slab at such shallow depths in the mantle. From the above 4 models it is evident that the bottom of the anomaly lies at depths between 660 km to 710 km barring HMSL-S06 which gives a maximum depth of 535 km. Assuming sinking rates of 10-12.5 $mmyr^{-1}$ in the upper mantle (Van der meer et al 2018), the models predict that the outlined anomaly subducted somewhere around 66-52.8 Ma (3D2016_09Sv), 68-54.4 Ma (GyPSuM-S), 53.5-42.8 Ma (HMSL-S06) and 71-56.8 Ma (SL2013sv). The lower limits for all of these age ranges except HMSL-S06 closely fit with timing of the Deccan event. The lower limit is accepted here as sinking rates of 12.5 $mmyr^{-1}$ have been documented in case of oceanic slabs which are denser than the continental roots. This marginally lower density of the continental root could result into descent rates which are comparable with the slab sinking rates, however not faster than the slabs themselves.

The following figure from opensource tomography database ATLAS of the underworld (Van der Meer et al 2018) which is a compilation of global high velocity seismic wave anomalies in the mantle, confirms that there are no

subducted slabs in the upper mantle and the mantle transition zone in the western Indian ocean enclosed by the square box in **Fig.9**.

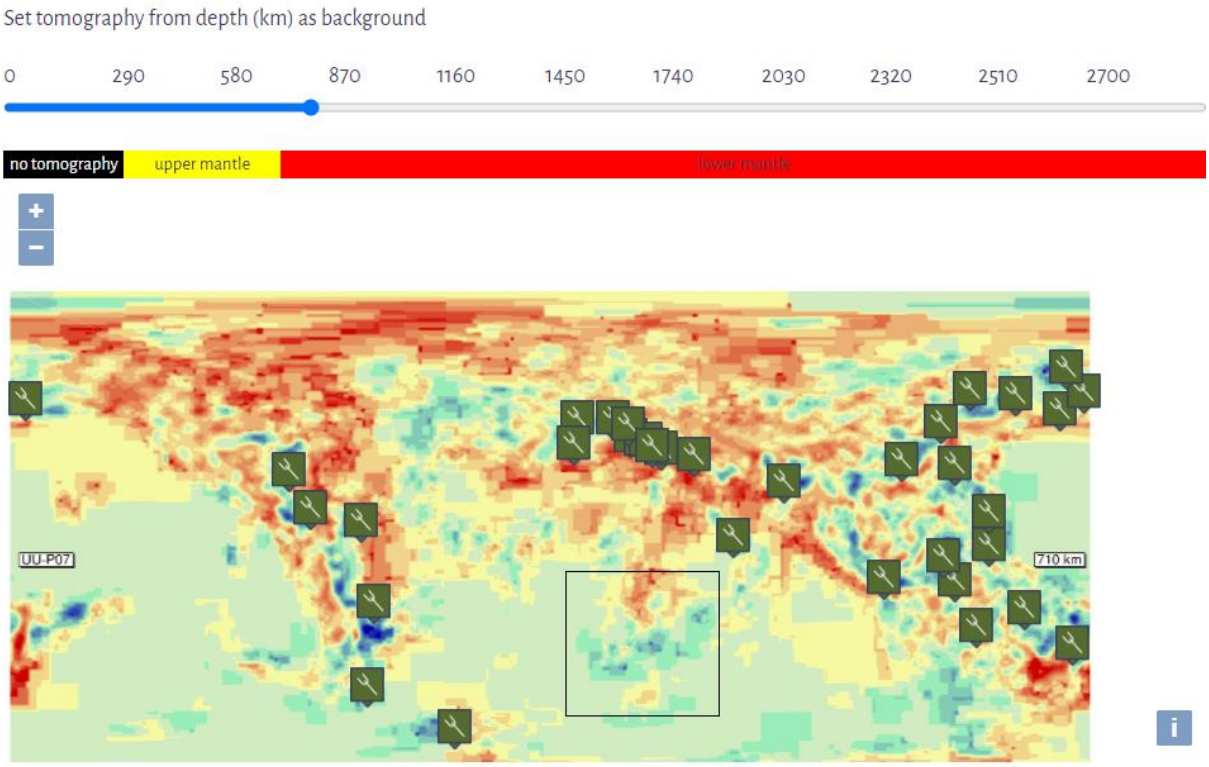


**Fig.9 Global seismic tomography map of the upper mantle at 710 km depth showing identified positive velocity anomalies in the upper mantle, where high velocity anomalies are depicted by the blue patches scattered throughout the globe. The box shows the region discussed in text where the bottom of the proposed delaminated lithosphere of the Indian subcontinent lies at depths of 660-710 km. Note the absence of any recognizable velocity anomalies to equate to oceanic lithospheric slabs stranded in the mantle in proposed region. The Carlsberg anomaly lying at depths between 800-1400 km is indicated by the pointer lying immediately to the NE of the box.**

Also, it is to be noted that the identified velocity anomaly should not be confused with the Carlsberg anomaly of Gaina et al (2015) which was identified to be the

record of a paleo-subduction in Late Mesozoic or Early Cenozoic southwest of the Himalaya resulting from an oblique subduction of Indian plate beneath the Arabian plate as is recorded in the Bela-Muslim Bagh-Waziristan-Kabul ophiolites; for the trends appear to be very identical. Another distinction is that the anomaly identified by Gaina et al (2015) lies entirely in the lower mantle between 800-1400 km. Whereas the present anomaly i.e. The Reunion anomaly, is still lying in the upper mantle and the mantle transition zone and has barely penetrated the lower mantle. The elongated and flat nature of the anomaly could be attributed to the convective stresses of the mantle flow in the upper mantle arising from the drag exerted by the Indian subcontinent and the Java-Sunda trench. We therefore propose that this anomalous body could possibly be the delaminated lithospheric root of the Indian subcontinent, which was mobilised by the Reunion plume resulting in reduced coupling between the Indian plate and the underlying asthenosphere. This loss of lithosphere effectively increased the efficiency of slab pull experienced by the Indian plate thereby resulting in enhanced velocities during and after the Deccan event.

Thus, from the above discussion, it appears very promising that the occurrence of a cold high-density anomaly exactly around Reunion latitudes with a geometry that does not resemble a subducted lithospheric slab and mantle sinking rates, that when backtracked lead to a delamination age of 66-70 Ma, which is precisely the age for Deccan-Reunion event could not be a mere coincidence. This therefore

strengthens the argument that the Indian subcontinent had lost a substantial portion of its cratonic root by the time it reached the Reunion latitudes which was further lessened during the Deccan event to a dismal thickness averaging only about 100-150 km along the peripheral reaches, and a maximum thickness of about 250 km in the Central Indian region along the Vindhyan basin. This mass deficit resulting from the loss of lithospheric material led to a decrease in the asthenospheric drag on the Indian plate, which combined with the slab pull and plume push forces resulted in tremendously high velocities.

## Conclusions

Paleogeographic reconstruction positions India in close proximity to spreading centres at the western and southern margins before the plume interaction at ~70-65 Ma (Van Hinsbergen et al 2019, Rodriguez et al 2021, Cande and Stegman 2011, Parsons et al 2021). The Indian subcontinent formed less than ~50% (roughly about 35-40%) of the total area of the Indian plate, which was dominantly comprised of oceanic lithosphere. Zahirovic et al (2015), explained based on numerical models that plates with a significant portion of the plate boundary involved in subduction zone experienced higher drift velocities compared to plates with no active subducting margins. If the subducting plate happens to carry a continental block, the size of the block would in turn decide the velocity of the moving plate. From the paleo-reconstructions it is obvious that Indian plate had a massive subduction zone at its northern boundary

(Hafkenschied et al 2004, Van der Meer et al 2018, Gibbons et al 2015) thereby placing an active propellant for the plate velocities.

Based on our calculations, we propose that the Indian subcontinent travelled at exceedingly high velocities which had never been recorded earlier directly. The Indian subcontinent experienced a brief pulse of hyper-spreading velocities when it encountered the Reunion plume-head (end of C30n to the end of C29n). The positive buoyancy created by the plume head combined together with the delamination of the lithosphere beneath India and the negative buoyancy due to Deccan basalt loading, both appear to have encouraged the larger displacements besides tilting of the continental block towards north by ~$10^0$. Once the plate moved away substantially from the plume head, lower velocities facilitated by lithospheric congealing are observed. The torques resulting from the multiple force vectors acting simultaneously are expressed by the clockwise/anticlockwise rotations and suitably derived from longitudinal and latitudinal drift components of the Indian plate at the same time. Thus, finally we report here one of the highest ever recorded plate velocities although for a short time span resulting from a combination of factors with changing intensities that modified plate movement including the directions precisely at 65$\pm$2 Ma.

## Declarations:

## Acknowledgements:

We acknowledge Ministry of Earth Sciences for funding through MoES/P.O.(Seismo)/1(353)/2018. All the authors acknowledge Head, Department of Geology SPPU, for support and encouragements. There are no conflicts of interests.

## References

Acharyya S.K., (2000). Break Up of Australia-India-Madagascar Block, Opening of the Indian Ocean and Continental Accretion in Southeast Asia With Special Reference to the Characteristics of the Peri-Indian Collision Zones, Gondwana Research, Volume 3, Issue 4, 2000, Pages 425- 43, ISSN 1342-937X, https://doi.org/10.1016/S1342-937X(05)70753-X.

Aitchison, J. C., Ali, J. R., and Davis, A. M. (2007), When and where did India and Asia collide? J. Geophys. Res., 112, B05423, doi:10.1029/2006JB004706.

Aitchison, J.C., Badengzhu, Davis, A.M., Liu, J.B., Luo, H., Malpas, J., McDermid, I.R., Wu, H., Ziabrev, S., & Zhou, M. (2000). Remnants of a Cretaceous intra-oceanic subduction system within the Yarlung-Zangbo suture (southern Tibet). Earth and Planetary Science Letters, 183, 231-244. DOI: 10.1016/S0012-821X(00)00287-9

Aitchison. J. C. and Davis A. M., Evidence for the multiphase nature of the India-Asia collision from the Yarlung Tsangpo suture zone, Tibet Geological Society, London, Special Publications, 226, 217-233, 1 January 2004, https://doi.org/10.1144/GSL.SP.2004.226.01.12

Amaru, M.L., 2007, Global travel time tomography with 3-D reference models: Geologica Ultraiectina, 274, 174p.

Argus, D. F., Gordon, R. G., and DeMets, C. (2011), Geologically current motion of 56 plates relative to the no-net-rotation reference frame, Geochem. Geophys. Geosyst., 12, Q11001, doi:10.1029/2011GC003751.

Bardintzeff. J. M. & Liégeois, J.-P & Bonin, Bernard & Bellon, Hervé & Rasamimanana, Georges. (2010). Madagascar volcanic provinces linked to the Gondwana break-up: Geochemical and isotopic evidences for contrasting mantle sources. Gondwana Research. 18. 295-314. 10.1016/j.gr.2009.11.010.

Baxter A.T., Aitchison J.C., Ali J.R., Chan J.S.L., Heung Ngai Chan G., Detrital chrome spinel evidence for a Neotethyan intra-oceanic island arc collision

with India in the Paleocene, Journal of Asian Earth Sciences, Volume 128, 2016, Pages 90-104, ISSN 1367-9120, https://doi.org/10.1016/j.jseaes.2016.06.023.

Bouilhol P., Jagoutz O., Hanchar J. M., Dudas O. F., Dating the India– Eurasia collision through arc magmatic records, Earth and Planetary Science Letters, Volume 366, 2013, Pages 163-175, ISSN 0012-821X, https://doi.org/10.1016/j.epsl.2013.01.023.

Buckman S. , Aitchison J.C., Nutman A.P., Bennett V.C., Saktura W. M., Walsh M.J.J, Kachovich S., Hidaka H., The Spongtang Massif in Ladakh, NW Himalaya: An Early Cretaceous record of spontaneous, intra-oceanic subduction initiation in the Neotethys, Gondwana Research, Volume 63, 2018, Pages 226-249, ISSN 1342-937X, https://doi.org/10.1016/j.gr.2018.07.003.

Cande S.C., Patriat P., Dyment J., Motion between the Indian, Antarctic and African plates in the early Cenozoic, Geophysical Journal International, Volume 183, Issue 1, October 2010, Pages 127–149, https://doi.org/10.1111/j.1365-246X.2010.04737.x

564 Cande. S. & Stegman. D. (2011). Indian and African Plate motions driven by the
565 push force of the Reunion plume head. Nature. 475. 47-52.
566 10.1038/nature10174.
567
568 Chenet A. L., Courtillot V., Fluteau F., Gérard M., Quidelleur X., Khadri S. F.
569 R., Subbarao K. V., Thordarson T. 2009 Determination of rapid Deccan
570 eruptions across the Cretaceous–Tertiary boundary using paleomagnetic
571 secular variation: 2. Constraints from analysis of eight new sections and
572 synthesis for a 3500-m-thick composite section; Journal of Geophysical
573 Research 114/38. doi: 10.1029/2008JB005644
574
575 Chenet A. L., Fluteau F., Courtillot V., Gerard M., Subbarao K.V. 2008
576 Determination of rapid eruption across the Cretaceous–Tertiary boundary
577 using paleomagnetic secular variation: Results from a 1200 m thick section
578 in the Mahabaleshwar escarpment; Journal of Geophysical Research 113
579 (B4), B04101.
580
581 Clennett, E. J., Sigloch, K., Mihalynuk, M. G., Seton, M., Henderson, M. A.,
582 Hosseini, K., et al. (2020). A quantitative tomotectonic plate reconstruction
583 of western North America and the eastern Pacific basin. Geochemistry,
584 Geophysics, Geosystems, 21, e2020GC009117.
585 https://doi.org/10.1029/2020GC009117

DeMets C, Merkouriev S, Detailed reconstructions of India–Somalia Plate motion, 60 Ma to present: implications for Somalia Plate absolute motion and India–Eurasia Plate motion, Geophysical Journal International, Volume 227, Issue 3, December 2021, Pages 1730–1767, https://doi.org/10.1093/gji/ggab295

Dessai A.G., Griffin W.L., Decratonization and reactivation of the southern Indian shield: An integrated perspective, Earth-Science Reviews, Volume 220, 2021, 103702, ISSN 0012-8252, https://doi.org/10.1016/j.earscirev.2021.103702.

Di-Cheng Zhu, Sun-Lin Chung, Xuan-Xue Mo, Zhi-Dan Zhao, Yaoling Niu, Biao Song, Yue-Heng Yang; The 132 Ma Comei-Bunbury large igneous province: Remnants identified in present-day southeastern Tibet and southwestern Australia. Geology 2009;; 37 (7): 583–586. Doi: https://doi.org/10.1130/G30001A.1

Dyment J., Evolution of the Carlsberg Ridge between 60 and 45 Ma: Ridge propagation spreading asymmetry and the Deccan-Reunion hotspot, Journal of Geophysical Research, vol. 103, no. B10, pages 24,067-24,084, October 10, 1998

Eagles G., Hoang Ha H., Cretaceous to present kinematics of the Indian, African and Seychelles plates, Geophysical Journal International, Volume 196, Issue 1, January 2014, Pages 1–14, https://doi.org/10.1093/gji/ggt372

Eagles G., Wibisono A. D., Ridge push, mantle plumes and the speed of the Indian plate, Geophysical Journal International, Volume 194, Issue 2, August 2013, Pages 670–677, https://doi.org/10.1093/gji/ggt162

Forsyth D., Uyeda S., On the Relative Importance of the Driving Forces of Plate Motion, Geophysical Journal International, Volume 43, Issue 1, October 1975, Pages 163–200, https://doi.org/10.1111/j.1365-246X.1975.tb00631.x

Gaina, C., van Hinsbergen, D. J. J., and Spakman, W. (2015), Tectonic interactions between India and Arabia since the Jurassic reconstructed from marine geophysics, ophiolite geology, and seismic tomography, *Tectonics*, 34, 875– 906. doi:10.1002/2014TC003780.

Georgen J. E., Lin J., Dick H. J. B., Evidence from gravity anomalies for interactions of the Marion and Bouvet hotspots with the Southwest Indian Ridge: effects of transform offsets, Earth and Planetary Science Letters,

629 Volume 187, Issues 3–4, 2001, Pages 283-300, ISSN 0012-821X,
630 https://doi.org/10.1016/S0012-821X(01)00293-X.
631
632 Ghatak A, Basu A. R., Vestiges of the Kerguelen plume in the Sylhet Traps,
633 Northeastern India, Earth and Planetary Science Letters, Volume 308,
634 Issues 1–2, 2011, Pages 52-64, ISSN 0012-821X,
635 https://doi.org/10.1016/j.epsl.2011.05.023.
636
637 Gibbons A.D., Zahirovic S., Müller R.D., Whittaker J.M., Yatheesh V., A
638 tectonic model reconciling evidence for the collisions between India,
639 Eurasia and intra-oceanic arcs of the central-eastern Tethys, Gondwana
640 Research, Volume 28, Issue 2, 2015, Pages 451-492, ISSN 1342-937X,
641 https://doi.org/10.1016/j.gr.2015.01.001.
642
643 Gibbons, A. D., Whittaker, J. M., and Müller, R. D. (2013), The breakup of East
644 Gondwana: Assimilating constraints from Cretaceous ocean basins around
645 India into a best-fit tectonic model, J. Geophys. Res. Solid Earth, 118, 808–
646 822, doi:10.1002/jgrb.50079.
647
648 Granot, R., Dyment, J. & Gallet, Y. Geomagnetic field variability during the
649 Cretaceous Normal Superchron. Nature Geosci 5, 220–223 (2012).
650 https://doi.org/10.1038/ngeo1404

Griffin W.L., A.F. Kobussen, E.V.S., Babu S.K., O'Reilly S. Y., Norris R., Sengupta P., A translithospheric suture in the vanished 1-Ga lithospheric root of South India: Evidence from contrasting lithosphere sections in the Dharwar Craton, Lithos, Volume 112, Supplement 2, 2009, Pages 1109-1119, ISSN 0024-4937, https://doi.org/10.1016/j.lithos.2009.05.015.

Gurnis M., Torsvik T. H.; Rapid drift of large continents during the late Precambrian and Paleozoic: Paleomagnetic constraints and dynamic models. Geology 1999; 22 (11): 1023–1026. Doi: https://doi.org/10.1130/00917613(1994)022<1023:RDOLCD>2.3.CO;2

Hafkenscheid, E., Wortel, M. J. R., and Spakman, W. (2006), Subduction history of the Tethyan region derived from seismic tomography and tectonic reconstructions, J. Geophys. Res., 111, B08401, doi:10.1029/2005JB003791.https://doi.org/10.31223/X5CS5N

Hall, R., Spakman, W. Mantle structure and tectonic history of SE Asia, Tectonophysics,Volume 658, 2015,Pages 14-45,ISSN 0040-1951, https://doi.org/10.1016/j.tecto.2015.07.003.

672 Ingle S., Weis D., Scoates J. S., Frey F. A., Relationship between the early
673 Kerguelen plume and continental flood basalts of the paleo-Eastern
674 Gondwanan margins, Earth and Planetary Science Letters, Volume 197,
675 Issues 1–2, 2002, Pages 35-50, ISSN 0012-821X,
676 https://doi.org/10.1016/S0012-821X(02)00473-9.
677
678 J.G. Ogg, Chapter 5 – Geomagnetic Polarity Time Scale, Editor(s): Felix M.
679 Gradstein, James G. Ogg, Mark D. Schmitz, Gabi M. Ogg, Geologic Time
680 Scale 2020, Elsevier, 2020, Pages 159-192, ISBN 9780128243602,
681 https://doi.org/10.1016/B978-0-12-824360-2.00005-X.
682
683 Jagoutz, O., Royden, L., Holt, A. et al. Anomalously fast convergence of India
684 and Eurasia caused by double subduction. Nature Geosci 8, 475–478
685 (2015). https://doi.org/10.1038/ngeo2418
686
687 Jaupart C., Mareschal J. C., The thermal structure and thickness of continental
688 roots, Lithos, Volume 48, Issues 1–4, 1999, Pages 93-114, ISSN 0024-
689 4937, https://doi.org/10.1016/S0024-4937(99)00023-7.
690
691 Jay A. E. and Widdowson M. 2008 Stratigraphy, structure and volcanology of the
692 south-easts Deccan continental flood basalt province: implications for

693 eruptive extent and volumes; Journal of the Geological Society London
694 165, 177-188.
695 Kale, V.S. (2020). Cretaceous Volcanism in Peninsular India: Rajmahal–Sylhet
696 and Deccan Traps. In: Gupta, N., Tandon, S. (eds) Geodynamics of the
697 Indian Plate. Springer Geology. Springer, Cham.
698 https://doi.org/10.1007/978-3-030-15989-4_8
699
700 Keller G., Nagori M. L, Chaudhary M, Reddy N.A., Jaiprakash B.C.,
701 Spangenberg Jorge E., Mateo P., Adatte T., Cenomanian-Turonian sea-
702 level transgression and OAE2 deposition in the Western Narmada Basin,
703 India, Gondwana Research, Volume 94, 2021, Pages 73-86, ISSN 1342-
704 937X, https://doi.org/10.1016/j.gr.2021.02.013.
705
706
707 Kumar, P., Yuan, X., Kumar, M. et al. The rapid drift of the Indian tectonic plate.
708 Nature 449, 894–897 (2007). https://doi.org/10.1038/nature06214
709
710 Kumari V., Tandon S.K., Kumar N., Ghatak A., Epicontinental Permian-
711 Cretaceous seaways in central India: The debate for the Narmada versus
712 Godavari rifts for the Cretaceous-Tertiary incursion, Earth-Science
713 Reviews, Volume 211, 2020, 103284, ISSN 0012-8252,
714 https://doi.org/10.1016/j.earscirev.2020.103284.

Lonsdale, P. (1983), Overlapping rift zones at the 5.5°S offset of the East Pacific Rise, J. Geophys. Res., 88( B11), 9393– 9406, doi:10.1029/JB088iB11p09393.

Malinverno, A., Quigley, K. W., Staro, A., & Dyment, J. (2020). A Late Cretaceous-Eocene geomagnetic polarity timescale (MQSD20) that steadies spreading rates on multiple mid-ocean ridge flanks. Journal of Geophysical Research: Solid Earth, 125, e2020JB020034. https://doi.org/10.1029/2020JB020034

Morgan, J.P. and Parmentier, E.M. (1984), Lithospheric stress near a ridge-transform intersection. Geophys. Res. Lett., 11: 113-116. https://doi.org/10.1029/GL011i002p00113

O'Neill C., Müller D., Steinberger B., Geodynamic implications of moving Indian Ocean hotspots, Earth and Planetary Science Letters, Volume 215, Issues 1–2, 2003, Pages 151-168, ISSN 0012-821X, https://doi.org/10.1016/S0012-821X(03)00368-6.

Olierook H. K. H, Jourdan F., Merle R. E., Timms N. E, Kusznir N., Muhling J. R., Bunbury Basalt: Gondwana breakup products or earliest vestiges of the Kerguelen mantle plume? Earth and Planetary Science Letters, Volume 440, 2016, Pages 20-32, ISSN 0012-821X, https://doi.org/10.1016/j.epsl.2016.02.008.

Parsons A. J., Hosseini K., Palin R. M., Sigloch K., Geological, geophysical and plate kinematic constraints for models of the India-Asia collision and the post-Triassic central Tethys oceans, Earth-Science Reviews, Volume 208, 2020, 103084, ISSN 0012-8252, https://doi.org/10.1016/j.earscirev.2020.103084.

Patriat, P., Achache, J. India–Eurasia collision chronology has implications for crustal shortening and driving mechanism of plates. Nature 311, 615–621 (1984). https://doi.org/10.1038/311615a0

Paul, J., and Ghosh, A., 2021, Could the Réunion plume have thinned the Indian craton?: Geology, v. XX, p. XXX–XXX, https://doi.org/10.1130/G49492.1

Pick, T., Tauxe, L. Geomagnetic palaeointensities during the Cretaceous normal superchron measured using submarine basaltic glass. Nature 366, 238–242 (1993). https://doi.org/10.1038/366238a0

Plummer, P.S. (1996), The Amirante ridge/trough complex: response to rotational transform rift/drift between Seychelles and Madagascar. Terra Nova, 8: 34-47. https://doi.org/10.1111/j.1365-3121.1996.tb00723.x

Poornachandra Rao G. V. S., Mallikharjuna Rao J., Palaeomagnetism of the Rajmahal Traps of India: Implication to the Reversal in the Cretaceous Normal Superchron, Journal of geomagnetism and geoelectricity, 1996, Volume 48, Issue 7, Pages 993-1000, Released on J-STAGE May 25, 2007, Online ISSN 2185-5765, Print ISSN 0022-1392, https://doi.org/10.5636/jgg.48.993,

Pusok A. E. and Stegman D. R. 2020 The convergence history of India-Eurasia records multiple subduction dynamics processes; Science Advances 6, eaaz8681.

Rodriguez M. The Amirante Ridge and Trench System in the Indian Ocean: the southern termination of the NW Indian subduction. Comptes Rendus. Géoscience, Volume 352 (2020) no. 3, pp. 235-245. doi : 10.5802/crgeos.40. https://comptes-rendus.academie-sciences.fr/geoscience/articles/10.5802/crgeos.40/

Rodriguez M., Arnould M., Coltice N., Soret M., Long-term evolution of a plume-induced subduction in the Neotethys realm, Earth and Planetary Science Letters, Volume 561, 2021, 116798, ISSN 0012-821X, https://doi.org/10.1016/j.epsl.2021.116798.

Sangode S. J., Dongre A., Bhagat A. R., Meshram D., Discovery of Deccan Inclination anomaly and its possible geodynamic implications over the Indian Plate (Article in Press: Journal of Earth System Sciences).

Schaeffer A. J., Lebedev S., Global shear speed structure of the upper mantle and transition zone, Geophysical Journal International, Volume 194, Issue 1, July 2013, Pages 417–449, https://doi.org/10.1093/gji/ggt095

800 Stoddard, P. R., and Abbott, D. (1996), Influence of the tectosphere upon plate
801 motion, J. Geophys. Res., 101( B3), 5425– 5433, doi:10.1029/95JB03540.
802 Storey, B. The role of mantle plumes in continental breakup: case histories from
803 Gondwanaland. Nature 377, 301–308 (1995).
804 https://doi.org/10.1038/377301a0
805 Talukdar, S.C., Murthy, M.V.N. The Indian traps, their tectonic history, and their
806 bearing on problems of Indian flood basalt provinces. Bull Volcanol 35,
807 602–618 (1971). https://doi.org/10.1007/BF02596831
808 Torsvik T.H, Tucker R.D, Ashwal L.D, Eide E.A, Rakotosolofo N.A, de Wit M.J,
809 Late Cretaceous magmatism in Madagascar: palaeomagnetic evidence for
810 a stationary Marion hotspot, Earth and Planetary Science Letters, Volume
811 164, Issues 1–2, 1998, Pages 221-232, ISSN 0012-821X,
812 https://doi.org/10.1016/S0012-821X(98)00206-4.
813 Van der Meer D.G., van Hinsbergen D. J. J., Spakman W., Atlas of the nderworld:
814 Slab remnants in the mantle, their sinking history, and a new outlook on
815 lower mantle viscosity, Tectonophysics, Volume 723, 2018, Pages 309-
816 448, ISSN 0040-1951, https://doi.org/10.1016/j.tecto.2017.10.004.
817 Van Hinsbergen, D. J. J. (2019). Comment on “Comparing paleomagnetic study
818 means with apparent wander paths: A case study and paleomagnetic test of
819 the Greater India versus Greater Indian Basin hypotheses” by David B.
820 Rowley. Tectonics, 38, 4516– 4520.
821 https://doi.org/10.1029/2019TC005525

Van Hinsbergen, D. J. J., Steinberger, B., Doubrovine, P. V., and Gassmöller, R. (2011), Acceleration and deceleration of India-Asia convergence since the Cretaceous: Roles of mantle plumes and continental collision, J. Geophys. Res., 116, B06101, https://doi:10.1029/2010JB008051.

Van Hinsbergen, D.J.J., Steinberger, B., Guilmette, C. et al. A record of plume-induced plate rotation triggering subduction initiation. Nat. Geosci. 14, 626–630 (2021). https://doi.org/10.1038/s41561-021-00780-7

Vandamme D., Courtillot V., Besse J., Montigny R. 1991 Palaeomagnetism and age determinations of the Deccan Traps (India); results of a Nagpur–Bombay traverse and review of earlier work; Reviews of Geophysics 29, 159–190.Volume 561,2021, 116798, ISSN 0012-821X, https://doi.org/10.1016/j.epsl.2021.116798

White L.T., Lister G.S., The collision of India with Asia, Journal of Geodynamics, Volumes 56–57, 2012, Pages 7-17, ISSN 0264-3707, https://doi.org/10.1016/j.jog.2011.06.006.

Zahirovic S., Müller R. D., Seton M., Flament N., Tectonic speed limits from plate kinematic reconstructions, Earth and Planetary Science Letters, Volume 418, 2015, Pages 40-52, ISSN 0012-821X, https://doi.org/10.1016/j.epsl.2015.02.037.

Zahirovic, S., Müller, R. D., Seton, M., Flament, N., Gurnis, M., and Whittaker, J. (2012), Insights on the kinematics of the India-Eurasia collision from

843 global geodynamic models, Geochem. Geophys. Geosyst., 13, Q04W11,
844 doi:10.1029/2011GC003883.